International Journal of Biological Macromolecules 261 (2024) 129701

Contents lists available at ScienceDirect

International Journal of Biological Macromolecules

journal homepage: www.elsevier.com/locate/ijbiomac

# Zein and hydroxypropyl methylcellulose acetate succinate microfibers combined with metronidazole benzoate and/or metronidazole-incorporated cellulose nanofibrils for potential periodontal treatment

João O. Ferreira [a], Giovana C. Zambuzi [a], Camilla H.M. Camargos [b,c], Ana C.W. Carvalho [d], Maíra P. Ferreira [d], Camila A. Rezende [b], Osvaldo de Freitas [d], Kelly R. Francisco [a,e,*]

[a] Science and Technology Center for Sustainability, Federal University of São Carlos, Rod. SP-264, km 110, Sorocaba 18052-780, SP, Brazil
[b] Department of Physical Chemistry, Institute of Chemistry, University of Campinas, 13083-970 Campinas, SP, Brazil
[c] School of Fine Arts, Federal University of Minas Gerais, 31270-901 Belo Horizonte, MG, Brazil
[d] Department of Pharmaceutical Sciences, Faculty of Pharmaceuticals Sciences of Ribeirao Preto, University of Sao Paulo, Ribeirao Preto 14040-903, SP, Brazil
[e] Department of Natural Science, Mathematics and Education, Federal University of São Carlos–UFSCar, Araras 13604-900, SP, Brazil

ARTICLE INFO

*Keywords:*
Electrospun fibers
Zein
Hydroxypropyl methylcellulose acetate succinate
Cellulose nanofibrils
Metronidazole benzoate
Metronidazole
Periodontitis

ABSTRACT

The development of flexible and porous materials to control antibacterial delivery is a pivotal endeavor in medical science. In this study, we aimed to produce long and defect-free fibers made of zein and hydroxypropyl methylcellulose acetate succinate (HPMCAS) to be used as a platform for the release of metronidazole (MDZ) and metronidazole benzoate (BMDZ) to be potentially used in periodontal treatment. Microfibers prepared via electrospinning under a 2:3 (w/w) zein to HPMCAS ratio, containing 0.5 % (w/w) poly(ethylene oxide) (PEO) and 1 % (w/w) cellulose nanofibril (CNF) were loaded with 40 % (w/w) MDZ, 40 % (w/w) BMDZ, or a combination of 20 % (w/w) of each drug. The addition of CNF improved the electrospinning process, resulting in long fibers with reduced MDZ and BMDZ surface crystallization. MDZ- and BMDZ-incorporated fibers were semi-crystalline and displayed commendable compatibility among drugs, nanocellulose and polymeric chains. Release tests showed that zein/HPMCAS/PEO fibers without CNF and with 20 % (w/w) MDZ/ 20 % (w/w) BMDZ released the drug at a slower and more sustained rate compared to other samples over extended periods (up to 5 days), which is a favorable aspect concerning periodontitis treatment.

## 1. Introduction

Periodontitis is a bacterial infectious disease that damages dental ligaments, leading to the formation of periodontal pockets due to detachment of the junctional epithelium and even the destruction of bones [1,2]. Periodontitis treatment requires scraping the bacterial plaque from these tissues concomitantly with application of antimicrobial agents, such as metronidazole, minocycline hydrochloride, azithromycin, chlorhexidine, and doxycycline [1–5]. Metronidazole is an antimicrobial with broad spectrum of action [6,7] and is also available as a prodrug, metronidazole benzoate (BMDZ), with a solubility ca. a hundred times lower than that of MDZ. The combined use of both in formulations is a good strategy to enhance the drug's residence time at the site of application.

Systemic administration of these antimicrobials causes adverse effects, prompting a shift towards local administration. The main challenge is to maintain a high drug concentration at the site for a prolonged period [7,8]. Mouthwashes and supragingival irrigations containing antimicrobials are ineffective in this regard as they do not penetrate the periodontal pocket [9] or are quickly washed by the crevicular fluid, with half of the drug eliminated within the first minute [10].

To maintain the necessary drug concentration in the periodontal pocket, a balance is required between the amount of drug released and the amount lost through leaching to the crevicular fluid or absorption into the bloodstream. An effective release system for this purpose must have a high initial drug load, providing a rapid release at the beginning

* Corresponding author at: Science and Technology Center for Sustainability, Federal University of São Carlos, Rod. SP-264, km 110, Sorocaba 18052-780, SP, Brazil.
*E-mail address:* kfrancisco@ufscar.br (K.R. Francisco).

https://doi.org/10.1016/j.ijbiomac.2024.129701
Received 5 July 2023; Received in revised form 13 January 2024; Accepted 22 January 2024
Available online 25 January 2024

("burst") of the treatment, followed by a slowed and sustained release rate as the flow of crevicular fluid decreases due to the drug effect on inflammation.

Different studies have investigated drug platforms suitable for treating periodontal diseases, including polymeric films, microspheres, gels, nanoparticles, and electrospun fibers [11–16]. In this scenario, electrospinning-produced fibers have received substantial attention as one can modulate their diameter (surface area), morphology, chemical composition, and density during the process, providing more flexible and mucoadhesive materials loaded with large amounts of active agents [8,17–25].

Despite such increasing portfolio of interesting studies on composite systems for treating periodontitis, research on the challenges related to controlling the drug releasing rate are still scarce. To fulfill the release requirements in both the beginning and later stages of the process, this study proposes loading the drugs with different ratios of hydrophobicity on electrospun fibers combining the hydrophobic polymer zein and the hydrophilic polymer HPMCAS [26,27].

As a water-insoluble polymer, zein is a good candidate for oral cavity insertion, serving as a platform for releasing MDZ and BMDZ molecules [28,29]. Moreover, zein electrospun fibers exhibit other attributes important for materials intended for this use, as softness, flexibility, comfort to the touch, and ease of handling, particularly when ethanol is used as a solvent. Yet, considering its poor mechanical and adhesive properties [30], the addition of other polymers should be explored to form improved composites.

Several studies have focused on obtaining electrospun fibers by blending hydroxypropyl methylcellulose (HPMC) with other macromolecules. [26,27,31–34]. Simultaneously, studies showed that the addition of cellulose nanofibrils (CNF) decreased the drug release rate on nanocellulose-containing films [35–38], suggesting that incorporating such nanoparticles into electrospun fibers can extend drug release while potentially assisting in the electrospinning process.

Herein we aimed to obtain defect-free, long cylindrical fibers to be used as a platform for the release of BMDZ (a hydrophobic drug) and MDZ (a hydrophilic drug), to potential treatment of periodontitis. For such, zein fibers were blended with HPMCAS and loaded with BMDZ, MDZ or a BMDZ/MDZ mix by electrospinning, while the effect of adding CNF to the electrospun composite fibers was also investigated. Assays on the drug release profiles were conducted in aqueous medium to mimic human saliva, allowing the calculation of drug release kinetics. Morphological investigations showed that CNF addition resulted in water-resistant fibers without defects (such as beads or film-formations), but nanocellulose decreased the release of BMDZ and MDZ. Given the adequate burst drug effect and prolonged and sustainable release achieved, the electrospun fibers comprising zein and HPMCAS with both drugs are potential drug delivery platforms for periodontitis treatment.

## 2. Experimental section

### 2.1. Materials

Zein 20 kDa, Poly(ethylene oxide) (PEO) 600 kDa, Metronidazole (MDZ) and Metronidazole benzoate (BMDZ) were purchased from Sigma/Aldrich. Hydroxypropyl methylcellulose acetate succinate (HPMCAS) 100 kDa was supplied by Ashland Inc. Ethanol 99.5 % was purchased from Synth. Cellulose nanofibrils (CNF) were produced from elephant grass leaves using TEMPO (2,2,6,6-tetramethylpiperidine-1-oxyl radical)-mediated oxidation followed by sonication [39]. CNF exhibited an elongated morphology (Fig. SM1), with an average length of 600 ± 300 nm, an average diameter of 10 ± 6 nm, and an aspect ratio of 100 ± 30 [39]. They are reported to be colloidally stable, with average zeta potentials as negative as – 60 mV, as also characterized in previous works [38,39]. Composite systems were prepared using a 30 % (w/w) water and 70 % (w/w) ethanol hydroalcoholic solution. All chemicals were applied as received. Milli-Q deionized water (resistivity: 18 MΩ cm) was used throughout the process.

### 2.2. Preparation of Zein/HPMCAS/CNF fibers

A hydroalcoholic solution (water/ethanol 3:7 (w/w)) containing 5 % (w/w) zein, 7.5 % (w/w) HPMCAS and 0.062 % (w/w) poly(ethylene oxide) (PEO) was prepared to result in a dried fiber mass of 39.8 % zein, 59.7 % (w/w) HPMCAS and 0.5 % (w/w) PEO, which correspondent to Zein:HPMCAS ratio of 2:3 (w/w). For the nanocellulose-containing systems, an aqueous CNF dispersion was added dropwise to the polymeric solutions under magnetic stirring for 1 h, as to achieve a 0.125 % (w/w) in the dispersion and 1.0 % (w/w) in the final dry weight of the fibers. MDZ and/or MDZ powder were added under magnetic stirring to the solution, in different proportions, to result in 7.99 % (w/w) of drugs in the solution and 40 % (w/w) in the dried fiber mass. The total solid content for dispersions without and with the drugs were approximately 12.7 % (w/w) and 19.4 % (w/w), respectively. Both MDZ and BMDZ were solubilized in the hydroalcoholic dispersions, although BMDZ had lower solubility and were not ready soluble. In this case, zein (hydrophobic polymer) played an important role in the solubilization/dispersion of BMDZ molecules for the electrospinning process.

Finally, the solutions or dispersions were placed in a 60 mL polypropylene syringe and pumped at a 4.0 mL $h^{-1}$ flow rate using a Samtronic® 670 – 39557D/28 syringe pump. The syringe was connected to a silicone tube, which was attached to a stainless-steel needle (⌀ = 1.20 mm) acting as a spinneret upper electrode to which a 15 kV voltage was applied. All needles were polarized using a ± 30 kV high voltage supply (Spellman CZE1000R). A square aluminum grounded counter electrode (10 × 10 $cm^2$) was covered with an aluminum foil to collect the fibers and placed 15.0 cm from the needle. Electrospinning experiments were performed inside a Faraday cage (1.00 × 1.00 × 0.60 $m^3$) to minimize external influences. Temperature (25 ± 2 °C) and relative humidity (55 ± 1 % RH) were monitored during the experiments using a MT-242 Minipa thermo-hygrometer. The produced fibers were kept in a desiccator for 72 h before measurement. Table 1 present the final composition of the solutions/dispersions and the final composition of the fibers.

The solubility of the fibers without the drugs was determined by the loss of mass due to the contact with a buffer solution at pH 7.0, resulting in solubility of 0.061 ± 0.003 (g $L^{-1}$) in the first 180 min and 0.091 ± 0.002 (g $L^{-1}$) in 24 h. The quantity of drugs on fibers was determined by separately placing samples of approximately 30 mg in 100 mL of 0.1 M sodium phosphate buffer (pH 7.0), which was remained in an ultrasound bath for 120 min. Drugs were then quantified by HPLC resulting in approximately 34.6 ± 2.7 % (w/w) of the drugs on the fibers. Tests were performed in quintuplicate.

**Table 1**
Composition (% w/w) of Zein/HPMCAS solutions/dispersions used to obtain the fibers and composition (% w/w) of Zein/HPMCAS fibers obtained by electrospinning, considering the total amount of the components.

| Solutions/dispersions (water/ethanol 3:7 (w/w)) | BMDZ | MDZ |
|---|---|---|
| 5.0 % Zein/ 7.5 % HPMCAS/ 0.062 % PEO | – | – |
| 5.0 % Zein/ 7.5 % HPMCAS/ 0.062 % PEO | 3.94 % | 3.94 % |
| 5.0 % Zein/ 7.5 % HPMCAS/ 0.062 % PEO / 0.125 % CNF | – | – |
| 5.0 % Zein/ 7.5 % HPMCAS/ 0.062 % PEO / 0.125 % CNF | 3.94 % | 3.94 % |
| 5.0 % Zein/ 7.5 % HPMCAS/ 0.062 % PEO / 0.125 % CNF | 7.99 % | – |
| 5.0 % Zein/ 7.5 % HPMCAS/ 0.062 % PEO / 0.125 % CNF | – | 7.99 % |
| **Fibers** | **BMDZ*** | **MDZ*** |
| 39.8 % Zein/ 59.7 % HPMCAS/ 0.5 % PEO | – | – |
| 23.9 % Zein/ 35.9 % HPMCAS/ 0.3 % PEO | 19.9 % | 19.9 % |
| 39.4 % Zein/ 59.1 % HPMCAS/ 0.5 % PEO/ 1.0 % CNF | – | – |
| 23.8 % Zein/ 35.7 % HPMCAS/ 0.3 % PEO/ 0.6 % CNF | 19.8 % | 19.8 % |
| 23.8 % Zein/ 35.7 % HPMCAS/ 0.3 % PEO/ 0.6 % CNF | 39.6 % | – |
| 23.8 % Zein/ 35.7 % HPMCAS/ 0.3 % PEO/ 0.6 % CNF | – | 39.6 % |

* Amount of drugs in % w/w considering the final dry mass of Zein/HPMCAS fibers.

### 2.3. Methods

#### 2.3.1. Zeta potential and conductivity of Zein/HPMCAS solutions/dispersions

Biopolymeric solutions or dispersions were placed in polystyrene cuvettes, and zeta potential and conductivity were measured at room temperature using a DLS Malvern Zetasizer Nano series Nano-ZS model ZEN3600.

#### 2.3.2. Rheology measurements of Zein/HPMCAS solutions/dispersions

Rheological experiments of polymeric solutions and dispersions were conducted on a Haake RheoStress 1 rheometer (Thermo Fisher Scientific) equipped with a plate-plate configuration (60 mm diameter, 1.0 mm gap). All flow curves were conducted in the shear rate from 0.05 to 100 $s^{-1}$ and all oscillatory experiments were carried out within the viscoelastic linear range with the frequency sweeps in the range of 0.01 to 10 Hz at 1 Pa. Experiments were performed using an external water-bath system at controlled temperature of 25.0 °C ± 0.1 °C.

#### 2.3.3. Scanning Electron Microscopy (SEM)

Fibers were fixed to the microscope sample holder and coated with an evaporated palladium-gold alloy using a Bal-Tec MED 020 Sputter. SEM analysis was performed on a Bruker Philips XL-30 FEG microscope operating at an acceleration voltage of 15 kV. SEM images were obtained by Secondary Electron Imaging (SEI) and Backscattered Electron Imaging (BEI).

The average diameter size of the fibers was estimated for a total of 100 randomly chosen points on the fibers of each sample using the Image J software (imagej.nih.gov) and the obtained values were statistically different. 02 SEM micrographs of the fibers with a scale bar of 20 μm were used to find the fiber diameters.

#### 2.3.4. Fourier Transform Infrared (FTIR)

FTIR spectra of zein/HPMCAS/CNF fibers with or without MDZ and BMDZ were obtained with a Bruker FT-IR Tensor II spectrometer, operating with ATR (attenuated total reflectance) accessory or the KBr insert holder. Spectra resulted of 128 scans within the spectral range of 500 to 4000 $cm^{-1}$ with a resolution of 4 $cm^{-1}$.

#### 2.3.5. X-ray Diffraction (XRD)

Fiber crystallinity was measured using a Rigaku MiniFlex X-ray diffractometer equipment with $CuK_{\alpha}$ radiation of 1.5418 Å, 40 kV and 30 mA. Diffractograms were obtained in the 2.0° to 70.0° range, with 10.0°$min^{-1}$ steps.

#### 2.3.6. Differential Scanning Calorimetry (DSC)

DSC curves for the fibers were obtained using a PerkinElmer 4000 equipment under nitrogen atmosphere at a 50 mL $min^{-1}$ flow rate, using hermetically sealed aluminum crucibles. Temperature was adjusted to −70 °C, kept constant for 10 min. Finally, the samples were heated from −70 °C to 230 °C at a 10 °C $min^{-1}$ heating rate.

#### 2.3.7. In vitro evaluation of the BMDZ and MDZ modified release profile

In vitro temperature-controlled (37 °C ± 2 °C) assays were performed using Franz-type vertical diffusion cells (volume = 30 mL, surface area = 4 $cm^2$) (Unividros, Ribeirão Preto, Brazil) with constant agitation at 300 rpm on a magnetic stirrer. A saline solution (pH 7.0) containing 0.16 mol $L^{-1}$ $Na_2HPO4$, 0.00138 M $KH_2HPO_4$, and 0.136 mol $L^{-1}$ NaCl was used as the receiving medium. The pH was adjusted to 7.0 using 0.1 mol $L^{-1}$ HCl or 0.1 mol $L^{-1}$ NaOH solutions. Previously hydrated cellulose ester membranes (Fisher Scientific®) (MWCO 0.5–2 kDa) were inserted between the donor and recipient compartments. A disc of surface area 1.71 $cm^2$ was weighted and placed in the donor cell compartment and the equivalent drug mass was calculated individually (approximately 10 mg of fibers, which corresponds to ca. 3.46 mg of the drugs). One mL aliquots of the receiving liquid were collected at predetermined times for the total time and the equivalent volume was replaced with a new solution. The experiment was performed over five days. Tests were performed in quintuplicate and under sink conditions.

Drug concentrations were measured by high-performance liquid chromatography (HPLC) (Shimadzu – PROEMINENCE), with UV diode array detector (DAD - model SPDM20A), reverse-phase column (C-18) Shim-pack VP-ODS model (4.6 mm × 25 cm), particle diameter of 5.0 μm, 313 K (40 °C), and 0.8 mL $min^{-1}$ flow rate. Mobile phase used methanol/ultrapure water 40:60 (v/v) in linear gradient mode (Methanol 40 % - 90 %), with injection volume of 20 μL and detection at 320 nm. Results were obtained using LabSolutions (Shimadzu) software. Sample concentrations were calculated by comparing curves constructed from metronidazole (MDZ) (FLUKA Sigma®) and metronidazole benzoate (BMDZ) (USP) primary standards using the straight-line regression equation $y = ax + b$, where 'y' is the peak area ratio, 'a' the slope, 'b' the intercept and 'x' the unknown drug concentration.

## 3. Results and discussion

### 3.1. Effect of PEO and Cellulose Nanofibril (CNF) on the formation of Zein/HPMCAS fibers

Relative humidity, temperature, surface tension, conductivity, and viscoelasticity of dispersions/solutions are important variables to consider when conducting electrospinning processes, as these properties influence the size and morphology of electrospun fibers [32,40–42].

In this study, we added a small amount of PEO (0.5 % (w/w)) 600 kDa to the Zein/HPMCAS solutions to enhance viscoelasticity and improve the quality of the produced fibers. [43,44] This approach was necessary as it was not possible to obtain fibers with the 5 % (w/w) Zein and 7.5 % (w/w) HPMCAS polymer solution (Fig. SM2). In fact, studies demonstrated that zein produced beaded fibers and other defects at low concentration and the addition of PEO in Zein or HPMC solutions improved the electrospinning process and the production of fibers with fewer defects [43,45–49].

Electrospinning of Zein/HPMCAS and PEO produced long cylindrical fibers without beads and an average diameter of 1.84 ± 0.44 μm (Fig. 1a). Conversely, electrospinning of Zein/HPMCAS and PEO loaded with 40 % (w/w) BMDZ produced fibers with an average diameter of 1.36 ± 0.40 μm. We observed drug crystallization into square and rectangular particles heterogeneously aggregated and distributed across the fiber surface (Fig. 1b). The crystallization was also observed for the fibers of Zein/HPMCAS and PEO loaded with 20 % (w/w) BMDZ and 20 % (w/w) MDZ, with an average diameter of 1.91 ± 0.57 μm (Fig. 1c).

Since decreasing drug crystallinity is essential to obtain good drug delivery platforms [27,31,32,50], we added a low amount of cellulose nanofibrils (CNF) to the Zein/HPMCAS and PEO solutions to obtain fibers with more BMDZ molecules incorporated into the polymeric matrix (Fig. 1d). BMDZ-loaded zein/HPMCAS/CNF fibers presented an average diameter of 2.17 ± 0.67 μm. The presence of few BMDZ crystals attached to the CNF-containing electrospun fiber surface indicates that drug crystallization occurred to a much lesser extent than in the fiber without CNF. The histograms obtained for the fiber diameters can be found in the Supplementary Material (Fig. SM3).

Fibers formed by two other Zein:HPMCAS ratios (3:2 (w/w) and 1:1 (w/w)) were also obtained. For instance, fibers formed by (i) 59.1 % (w/w) Zein/ 39.4 % (w/w) HPMCAS/ 0.5 % (w/w) PEO/ 1.0 % (w/w) CNF and its correspondent fiber with the drugs (35.7 % (w/w) Zein/ 23.8 % (w/w) HPMCAS/ 0.3 % (w/w) PEO/ 0.6 % (w/w) CNF and 39.6 % (w/w) drugs), and fibers of (ii) 49.2 % (w/w) Zein/ 49.2 % (w/w) HPMCAS/ 0.5 % (w/w) PEO/ 1.0 % (w/w) CNF and the correspondent fibers with drugs (29.7 % (w/w) Zein/ 29.7 % (w/w) HPMCAS/ 0.3 % (w/w) PEO/ 0.6 % (w/w) CNF and 39.6 % (w/w) drugs). However, those fibers were not appropriated to be used as drug platform as they presented many defects, for instance beads, regions forming films and fibers with great variance in the diameter (very thin and thick fibers in the same sample),

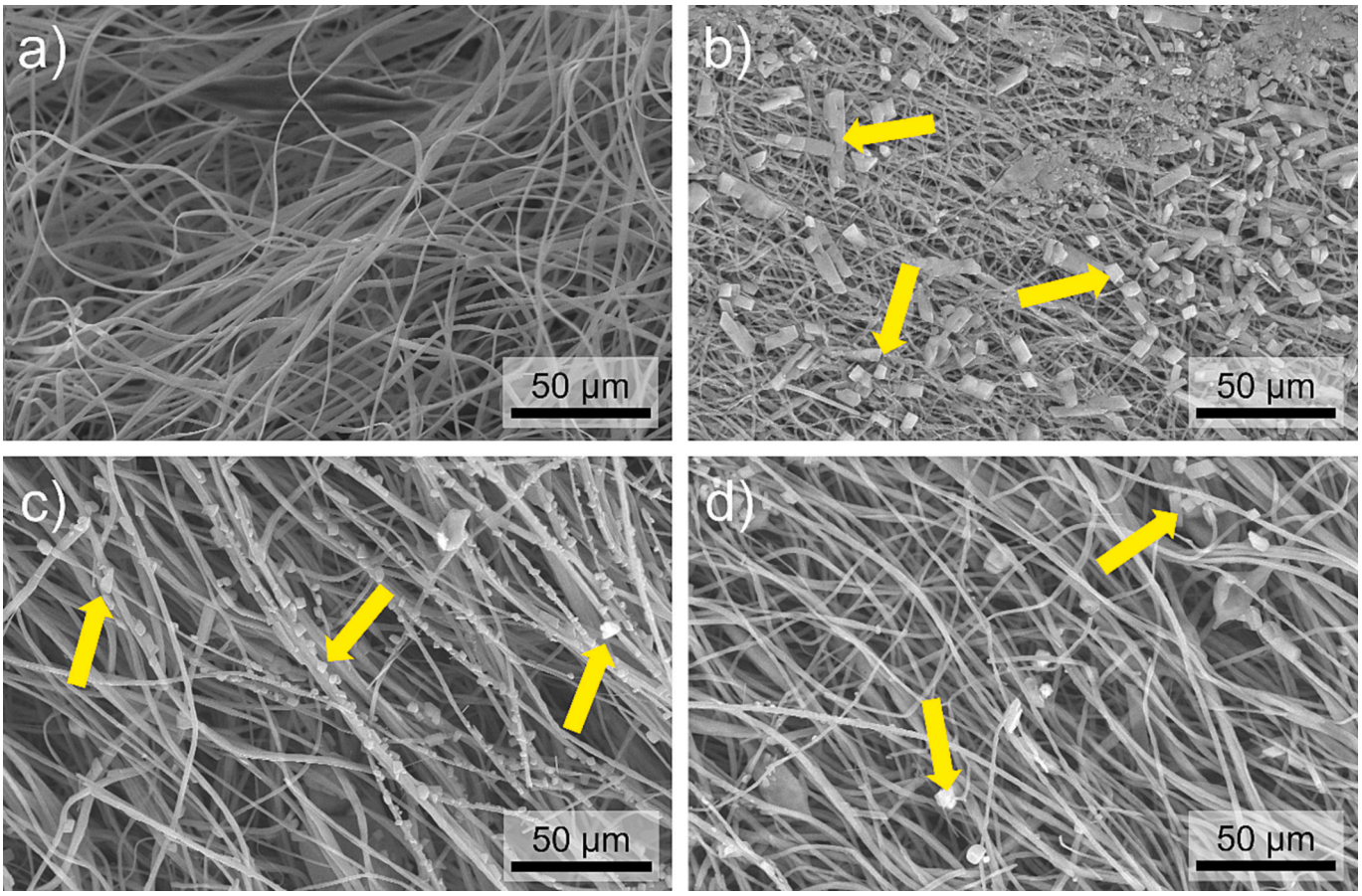


**Fig. 1.** SEM surface images for (a) Zein/HPMCAS/PEO fibers, (b) Zein/HPMCAS/PEO fibers with BMDZ, (c) Zein/HPMCAS/PEO fibers with BMDZ and MDZ, and (d) Zein/HPMCAS/PEO/CNF fibers with BMDZ. Yellow arrows in (b), (c), and (d) indicate drug particles and aggregates. Scale bars: 50 μm.

which can be observed in the Supplementary Material (Fig. SM4).

In this study, microfibers were produced instead of nanofibers probably due to the hydroalcoholic solutions formed by ethanol have low superficial tension and/or low charge density values of the electrified jet and, consequently, thicker fibers were produced when compared to the fibers obtained using water as a solvent, as it was reported elsewhere [51–55]. Although fibers were obtained on a microscale, the membrane produced was suitable to be used as a potential platform for the release of BMDZ and/or MDZ.

The addition of CNF particles also played an important role in the viscoelasticity of the Zein/HPMCAS dispersions, and, consequently in the electrospinning process and in the quality of produced fibers (Table 2). Results of zeta potential and conductivity (Table 2) showed similar values for all Zein/HPMCAS solutions or dispersions, suggesting that these properties were not the main factor in obtaining Zein/HPMCAS fibers. However, the zero-shear viscosity ($\eta_0$) of the systems presented significant differences.

**Table 2**
Zeta potential, conductivity and zero-shear viscosity of the polymeric solutions and dispersions with and without the drugs.

| Solution/dispersion % (w/w) | Zeta potential (mV) | Conductivity (μS/cm) | $\eta_0$ (Pa.s) |
|---|---|---|---|
| Zein/HPMCAS/PEO | −0.518 ± 0.069 | 533.0 ± 32.4 | 5.146 |
| Zein/HPMCAS/PEO/7.99 % BMDZ | −0.459 ± 0.037 | 461.0 ± 26.3 | 0.721 |
| Zein/HPMCAS/PEO/3.94 % BMDZ/ 3.94 % MDZ | −0.474 ± 0.050 | 443.0 ± 20.1 | 1.100 |
| Zein/HPMCAS/PEO/CNF | −0.484 ± 0.034 | 528.0 ± 32.7 | 10.267 |
| Zein/HPMCAS/PEO/CNF/7.99 % BMDZ | −0.435 ± 0.035 | 487.0 ± 21.0 | 15.803 |
| Zein/HPMCAS/PEO/CNF/3.94 % BMDZ/ 3.94 % MDZ | −0.417 ± 0.024 | 455.0 ± 24.3 | 22.788 |
| Zein/HPMCAS/PEO/CNF/7.99 % MDZ | −0.423 ± 0.031 | 498.0 ± 28.9 | 10.918 |

Generally, the electrospinning process is facilitated by high values of zero-shear viscosity due to the entanglements formed between polymeric chains, leading to a high viscoelastic fluid [45,46,56]. Thus, Zein/HPMCAS solutions or dispersions with low $\eta_0$ values may present poor electrospinnability and/or formation of fibers with beads or other defects. In this case, the addition of BMDZ molecules in Zein/HPMCAS/PEO solution led to a lower $\eta_0$ value compared to the solution without the drug, for instance, $\eta_0$ was 7 times smaller for the system with the drug, and BMDZ crystallization was observed on the polymeric fiber surface (Fig. 1 *b*).

On the other hand, the addition of small amount of nanocellulose in the Zein/HPMCAS/PEO solutions with and without the drug increased the $\eta_0$ values by at least 2 times, and a lower content of drug-crystallization were observed on the fibers (Fig. 1 *c*). Comparing $\eta_0$ values of the solution/dispersions with the diameters of the fibers shown in Fig. 1 *a*, *b,* and *c*, it is noticeable that a lower $\eta_0$ corresponds to a smaller diameter. This relationship holds true even though the dispersion of Zein/HPMCAS/PEO with BMDZ presented a higher total solid content (19.4 % (w/w)) compared to the solution without the drug (12.7 % (w/w)). The dispersion of Zein/HPMCAS/PEO/CNF with BMDZ exhibited the highest $\eta_0$ value, resulting in fibers with the largest diameter.

Furthermore, the addition of nanocellulose in Zein/HPMCAS/PEO solutions increased the viscoelasticity of the system, since storage

modulus (*G'*) values are higher than lost modulus (*G''*) as a function of frequency (*f*) for Zein/HMPCAS/PEO/CNF compared to the Zein/HPMCAS/PEO solution. These results can be found in the Supplementary Material (Fig. SM5). The higher G' value, the more viscoelastic the fluid becomes, and the G'/G" curves for this system resemble a viscoelastic system formed by polymers or wormlike micelles in a semi-diluted solution [57,58].

This result suggests that CNF can act as physical crosslinkers between zein and/or HPMCAS chains, leading to a more effective entanglement and network formation due to the intermolecular interactions formed among the macromolecules, primarily via hydrogen bonds [59–64]. A higher density of entanglements results in increased viscosity values ($\eta_0$) (Table 2), and the polymeric dispersions become more viscoelastic, facilitating the electrospinning process and allowing a more adequate drug impregnation. Indeed, CNF addition can both increase the viscoelasticity of the dispersion and improve the interaction between the polymeric chains and the drugs, decreasing drug crystallinity and influencing their release behavior [35,36]. Moreover, adding CNF is a more suitable strategy to obtain fibers with lower solubility than using higher amounts of PEO, since this polymer is highly water soluble,

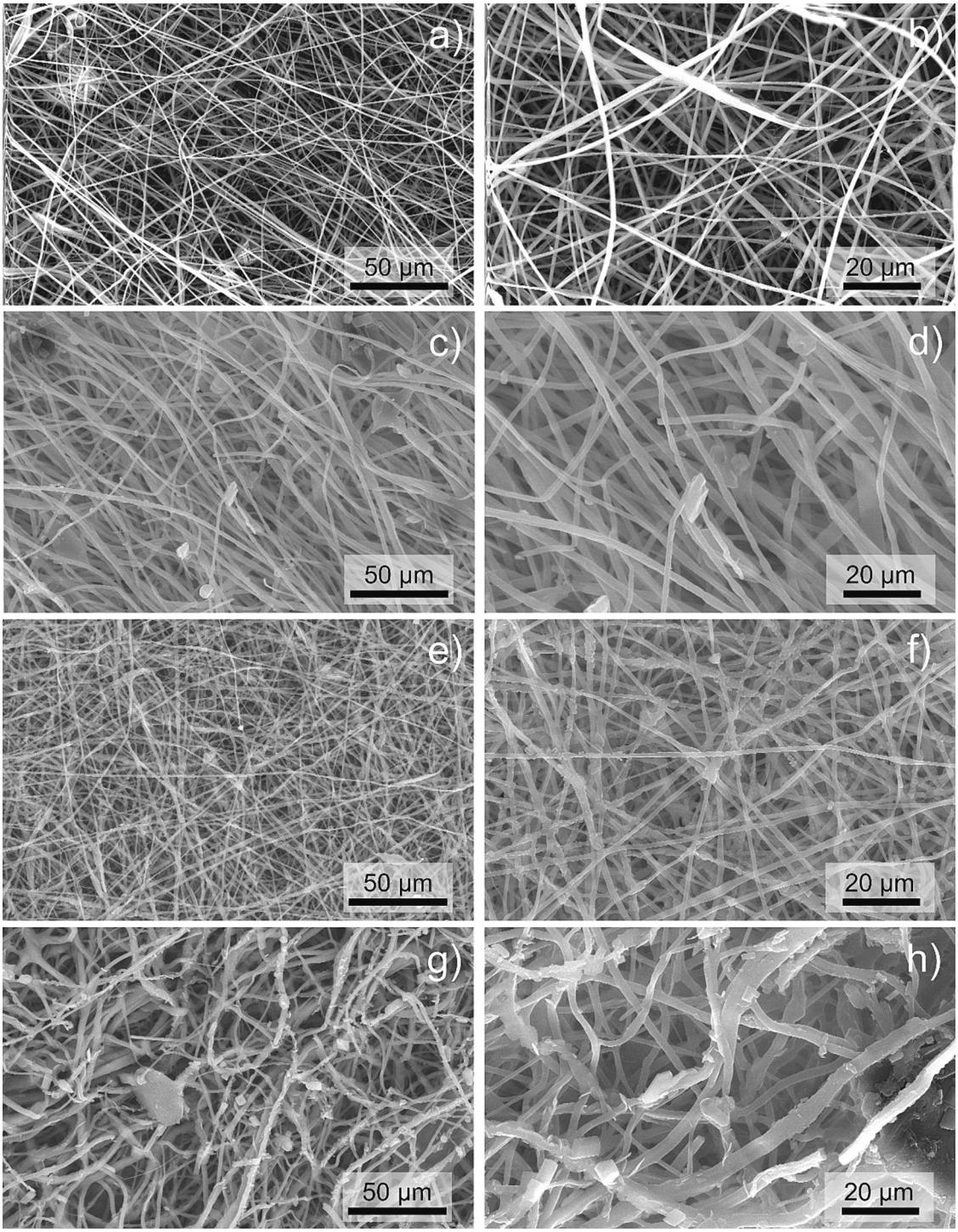


**Fig. 2.** SEM images of Zein/HPMCAS/CNF (a, b) alone and loaded with (c, d) 40.0 % (w/w) BMDZ, (e, f) 40.0 % (w/w) MDZ, and (g, h) 20.0 % (w/w) BMDZ +20.0 % (w/w) MDZ. Scale bars: (a, c, e, g) 50 μm and (b, d, f, h) 20 μm.

producing less stable drug platforms for aqueous media.

Considering these findings, we proceeded with characterizing the Zein:HPMCAS ratio of 2:3 (w/w), i.e., 39.4 % (w/w) Zein/ 59.1 % (w/w) HPMCAS/ 0.5 % (w/w) PEO/ 1.0 % (w/w) CNF fibers without drugs or loaded with different amounts of BMDZ and/or MDZ molecules (fibers composition of 23.8 % Zein (w/w)/ 35.7 % (w/w) HPMCAS/ 0.3 % (w/w) PEO/ 0.6 % (w/w) CNF and 39.6 % (w/w) drugs). We also investigated the effects of adding nanocellulose on the release kinetics and the BMDZ and MDZ release curves.

### *3.2. Morphological, chemical, and thermal characterization of Zein/HPMCAS/CNF fibers with or without drugs*

To investigate the morphology of Zein/HPMCAS/CNF fibers, alone or loaded with mobilized drugs, we obtained SEM images at two different magnifications (Fig. 2). The histograms obtained for the Zein/HPMCAS/CNF fibers diameter are in the Supplementary Material (Fig. SM3).

SEM images of composite fibers alone (Fig. 2a, b) showed long randomly oriented cylinders with diameter of 1.32 ± 0.29 μm, without granules and with a smooth surface. The addition of 40 % (w/w) BMDZ (Fig. 2c, d), 40 % (w/w) MDZ (Fig. 2e, f), and 20 % (w/w) BMDZ/ 20 % (w/w) MDZ (Fig. 2g, h) resulted in long fibers with diameters of 2.13 ± 0.56, 1.54 ± 0.33, and 2.31 ± 0,68 μm respectively, without beads but with some aggregates and drug crystals. The fiber diameters of Zein/HPMCAS/PEO/CNF with and without the drugs also increased with the increment of $\eta_0$ values of the dispersions (Table 2). Moreover, the membrane loaded with BMDZ and MDZ molecules (Fig. 2g, h) showed fibers less uniform in diameter and exhibiting a rougher surface when compared with the composite fibers with a single type of drug loaded into the polymer matrix (Fig. 2c–f).

However, even for the BMDZ/MDZ-loaded fibers, the high content of incorporated drugs was not detrimental to the composite cohesion, as only a small amount of drug crystals was formed on their surface. Xue et al. [23] observed similar trends for drug crystallization on the fiber surface of systems containing 20 % (w/w) metronidazole mobilized in polycaprolactone fibers. In turn, He et al. [24] observed that fibers formed by polycaprolactone and zein presented MDZ crystals in loads superior to 20 % (w/w). Thus, our findings indicate that adding cellulose nanofibrils proved to be an efficient strategy for producing Zein/HPMCAS/CNF membranes for BMDZ and/or MDZ release at higher concentrations than usually reported in the literature. CNF contributed to both the electrospinning and drug incorporation.

FTIR spectra of individual components are shown in Supplementary Material (Fig. SM6) and they presented the typical bands for the pristine polymers and drugs. FTIR spectra of Zein/HPMCAS/CNF fibers loaded with different amounts of BMDZ and MDZ are shown in Fig. 3.

Main adsorption bands in the spectra for the electrospun fibers (Fig. 3), particularly those located at 3500–3000 $cm^{-1}$ and 1700–1600 $cm^{-1}$, presented shifts in wavenumber and changes in relative areas as compared to the pure components (Fig. SM6). Zein/HPMCAS fibers without drugs presented a broad band centered at 3305 $cm^{-1}$ due to the overlapping of N—H and O—H stretching vibrations, which were shifted to lower wavenumbers, suggesting intermolecular interactions among polymeric chains and the nanoparticles [64,65,68]. The CNF-fiber containing 40.0 % (w/w) BMDZ showed similar profile compared to the membrane without drugs, except by the shift of the mentioned band towards 3292 $cm^{-1}$, indicating changes in the hydrogen bond interactions among BMDZ and the macromolecules.

The addition of MDZ molecules leads to the overlapping of this band, with a sharp band at 3215 $cm^{-1}$ being attributed to the presence of this drug into the electrospun CNF-fiber. Moreover, there were shifts towards higher wavenumbers for bands related to amide I (1700–1600 $cm^{-1}$) of the zein structure. A band attributed to amide I was observed at 1651 $cm^{-1}$ for the fiber without drug and at 1654, 1655, 1652 and 1654 $cm^{-1}$ for CNF-fibers containing 40.0 % (w/w) BMDZ, 40.0 % (w/w) MDZ, 20.0 % (w/w) BMDZ/ 20.0 % (w/w) MDZ and for fibers without CNF containing the drugs, respectively. This band was shifted by about 12–16 $cm^{-1}$ compared to pure zein, phenomenon assigned to the predominant presence of zein in the α-helix structure and increased disordered β-sheets [64,65]. No significant shifts were observed for other typical or fingerprint absorption bands, indicating that the polymers and drugs remained stable during the electrospinning process, with only specific intermolecular interactions occurring among the components.

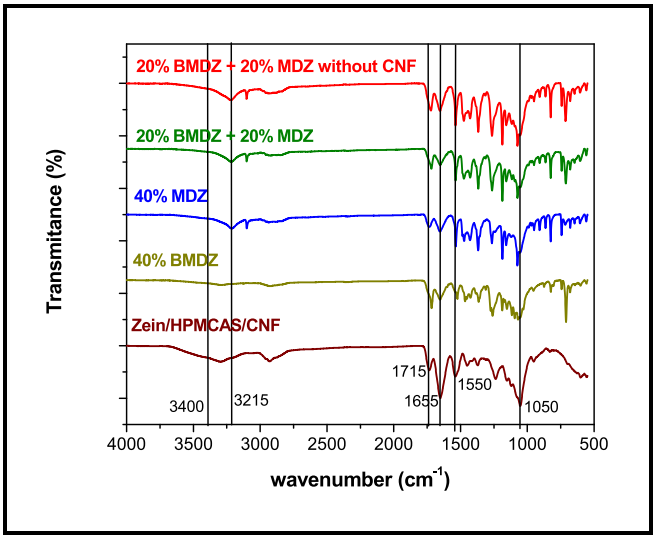


**Fig. 3.** FTIR spectra of Zein/HPMCAS/PEO and Zein/HPMCAS/PEO/CNF electrospun fibers: without drugs or loaded with 40.0 % (w/w) BMDZ, 40.0 % (w/w) MDZ, or 20.0 % (w/w) BMDZ + 20.0 % (w/w) MDZ.

Fig. 4a shows the XRD pattern of pristine components. Zein powder presented typical broad peaks at 2θ = 9.7° (10.1 Å distance) and 20.1° (4.9 Å distance), related to the inter-α-helix packing and the backbone distance of the macromolecular chains, respectively [27]. XRD diffractograms for HPMCAS fibers revealed broad peaks around 2θ = 11.4° (8.6 Å distance) and 19.5° (5.1 Å distance) [65]. Conversely, the crystalline drugs showed characteristic well-defined diffraction peaks at 11.4° (8.6 Å distance) and 13.5° (7.3 Å distance) for BMDZ samples [66] and at 12.2° (8.1 Å distance) and 13.8° (7.1 Å distance) for MDZ samples [23], among other various sharp and intense peaks. These findings confirmed that the macromolecules exhibit a semicrystalline to amorphous nature, while both drugs show high crystallinity in their native form. Diffractograms of electrospun Zein/HPMCAS/CNF fibers alone or loaded with drugs presented important differences between each other and when compared with the pure components (Fig. 4b).

Drug-free electrospun fiber showed diffraction halos centered at 2θ = 9.7° and 20.9°. Drug-loaded fibers formed semicrystalline materials, presenting some peaks related to the presence of BMDZ (12.0°, 19.3°, 22.0°, 25.0°) and/or MDZ (12.4°, 13.96°, 19.6°, 25.6°, 27.8°), a slight shift when compared with data for pure drugs and overlapping with the amorphous halo of Zein/HPMCAS/CNF samples. We also observed a substantial decrease in the number and intensity of these peaks, indicating that the crystallinity of both drugs decreased during electrospinning due to intermolecular interactions between polymeric chains and drug molecules, namely electrostatic interactions and hydrogen bonds, as previously reported for other drugs mobilized on different polymer platforms [38,67]. Crystallinity and stability of the drugs during electrospinning were verified by DSC of the fibers (Fig. 5).

DSC curves of pure zein and HPMCAS (Fig. 5a) showed a broad endothermic peak at 80.3 °C and 71.9 °C, respectively, attributed to the evaporation of water molecules trapped within their chains [24,32] Moreover, the glass transition temperatures of zein and HPMCAS were approximately 170 and 140 °C, respectively, and the endothermic peak at 280 °C observed on the zein DSC curve is due to its degradation [68].

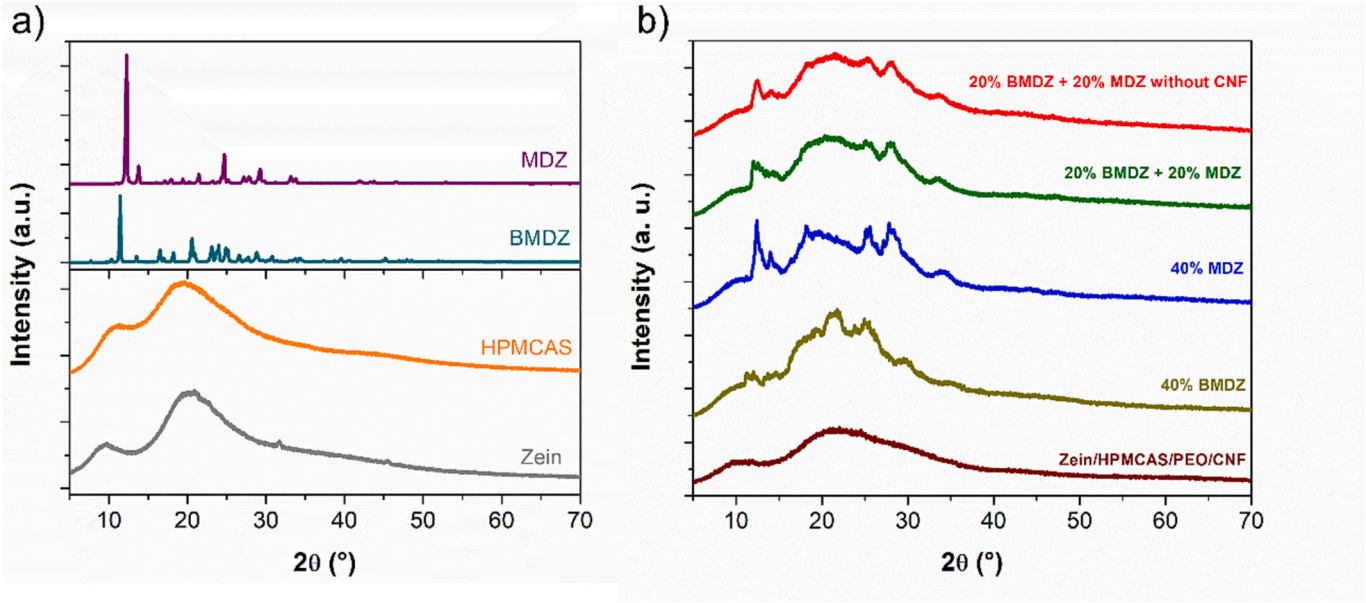


**Fig. 4.** XRD patterns of (a) pure components: zein, HPMCAS, BMDZ, and MDZ, and (b) Zein/HPMCAS/PEO fiber without or with CNF; the later were loaded with 40.0 % (w/w) BMDZ, 40.0 % (w/w) MDZ, 20.0 % (w/w) BMDZ + 20.0 % (w/w) MDZ or did not contain any drug.

Conversely, the sharp endothermic peaks at 103.8 and 168.5 °C on the DSC curves for BMDZ and MDZ, respectively, were attributed to their melting point, according to their XRD-verified crystalline profile [20,29]. DSC thermograms of Zein/HPMCAS/CNF fibers (Fig. 5b) showed a broad endothermic peak at 61.1 °C, similar to that observed for pure zein and HPMCAS compounds, and is also attributed to the evaporation of unbound water molecules adsorbed on the polymeric composite.

Zein/HPMACS/CNF fibers loaded with 40 % (w/w) BMDZ, 40 % (w/w) MDZ and 20 % (w/w) BMDZ/20 % (w/w) MDZ showed a small endothermic peak at 99.6, 146.3, and 127.3 °C, respectively, due to melting of the drug crystals. When incorporated into the electrospun fibers, the melting point of both drugs showed a significant decrease. Temperature values changed from 103.8 to 99.6 °C for BMDZ and from 168.5 to 146.3 °C for MDZ, suggesting a good intermolecular interaction between drug molecules and polymer chains [29].

Moreover, the fibers loaded with 20 % (w/w) of each drug showed a single peak, indicating strong intermolecular interactions between both drugs and between the macromolecules, since the melting point of the drug in the fiber decreased considerably compared with the melting point of pure MDZ and no peak related to BMDZ molecules was observed. All drug-loaded fibers showed exothermic peaks at around 285 °C related to membrane degradation/oxidation, regardless of the chemical structure of the drug [29].

### 3.3. Modified drug release

Differences in the diameter, roughness, surface area, component proportions, and intermolecular interactions of electrospun fibers can influence the mechanism and rate of drug release from membranes in an aqueous medium. Fig. 6a shows the release of BMDZ and/or MDZ from Zein/HPMCAS/CNF (with cellulose nanofibrils) or Zein/HPMCAS (without CNF) electrospun fibers. The drug percentage is related to the total amount of BMDZ and/or MDZ in the polymeric matrix. These values are also presented in Table SM1 in the Supplementary Material.

The release profiles of BMDZ and MDZ molecules from polymeric fibers showed different characteristics depending on the drug release stage. At short times up to 1 h, drug release from CNF-containing fibers was approximately 11, 77, and 32 % (w/w) for the material loaded with 40 % (w/w) BMDZ, 40 % (w/w) MDZ and 20 % (w/w) BMDZ/ 20 % (w/w) MDZ, respectively; and 32 % (w/w) for membranes containing 20 % (w/w) BMDZ/ 20 % (w/w) MDZ without nanocellulose. CNF-containing fibers loaded with only BMDZ molecules had slower drug release in short times whereas the equivalent electrospun membranes with 40 % (w/w) MDZ showed a drug burst effect, as reported by other authors [8,29,69]. At long times (up to 48 h), drug release values were 71, 81, and 55 % (w/w) for Zein/HPMCAS/CNF membranes loaded with 40 % (w/w) BMDZ, 40 % (w/w) MDZ and 20 % (w/w) BMDZ/ 20 % (w/w) MDZ, respectively, and 83 % (w/w) for Zein/HPMCAS fibers loaded with a 20 % (w/w) mixture of each drug. By this time (48 h), the release of drugs from these three formulations with CNF particles had already stopped.

The fibers obtained with the addition of CNF showed better quality, with a more uniform and smoother surface as (Fig. 1c) compared to fibers without the addition of CNF (Fig. 1b). However, the release of drugs from formulations containing CNF reached a plateau after 48 h (Fig. 6a), indicating that there was no further release of drugs. None of the formulations with CNF reached a 100 % (w/w) release, suggesting that CNF, despite guaranteeing the quality of the fibers, hindered the total release of the drugs. On the other hand, despite their low quality, the fibers without the addition of CNF enabled the release of the drugs during the 5 days of experiment, without reaching a plateau, and thus demonstrating a release profile suitable for the proposed purpose.

Fig. 6b provides a closer look at the release profile of individual drugs from Zein/HPMCAS/CNF or Zein/HPMCAS fibers loaded with 20 % (w/w) BMDZ/ 20 % (w/w) MDZ. The drug release values at 30 min, 1 h, 6 h, and 48 h are also presented in Table SM2 in the Supplementary Material. It is possible to state that the use of the two drugs MDZ and BMDZ, concomitantly in the systems, allows obtaining the bimodal release profile, suitable for the proposed system. In the first hours of the experiment, MDZ is quickly released, allowing rapid initial action of the drugs and then BMDZ is released more slowly, allowing the maintenance of release and prolonged effect of the drugs up to 48 h for the formulation with CNF and up to 5 days for those without CNF.

The appropriated drug release rate is related to the use of the minimum concentration of the drug that is effective against a specific pathogenic agent during the treatment [3,20,24,25,69]. For instance, Reise et al. [25] verified that electrospun polyactide (PLA) fibers using acetone as solvent and with 0.1–40 % (w/w) MDZ presented antibacterial efficacy for *A. actinomycethemcomitans, P. gingivalis and F.*

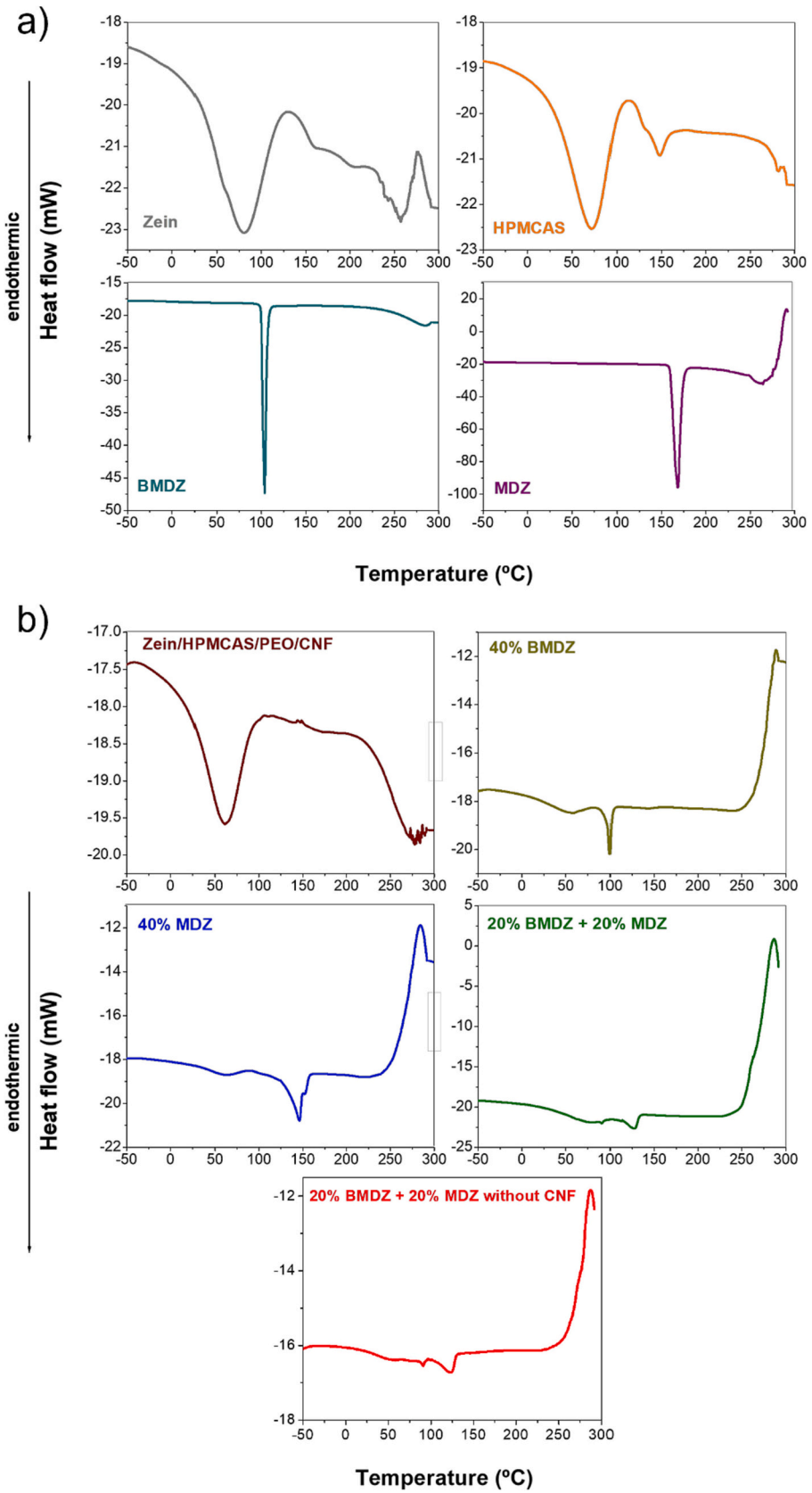


**Fig. 5.** DSC curves of (a) pure components: zein, HPMCAS, BMDZ, and MDZ, and (b) Zein/HPMCAS/PEO and Zein/HPMCAS/PEO/CNF fibers: alone or loaded with 40.0 % (w/w) BMDZ, 40.0 % (w/w) MDZ, and 20.0 % (w/w) BMDZ + 20.0 % (w/w) MDZ.

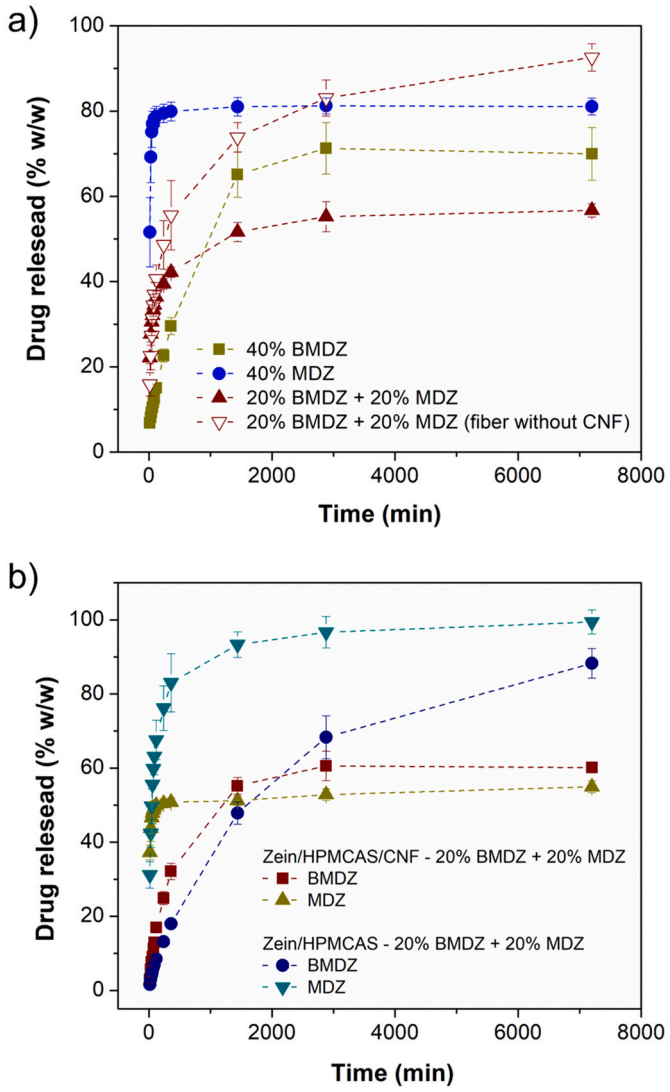


**Fig. 6.** BMDZ and MDZ release profile: (a) Drug molecules were mobilized on electrospun Zein/HPMCAS/CNF at different concentrations: 40.0 % (w/w) BMDZ, 40.0 % (w/w) MDZ, and 20.0 % (w/w) BMDZ + 20.0 % (w/w) MDZ; and specifically at 20.0 % (w/w) BMDZ + 20.0 % (w/w) MDZ onto Zein/HPMCAS fibers (without CNF); (b) Individual drug release profile of BMDZ and MDZ mobilized in Zein/HPMCAS/CNF or Zein/HPMCAS fibers containing 20 % (w/w) of each drug mixed.

*nucleatum,* that have the minimal inhibitory concentrations of 256 μg/mL, 0.031–1.5 μg/mL and approximately 0.030 μg/mL, respectively. 2 mg fibers loaded with 10.0–40 % (w/w) MDZ with at least 10 % (w/w) release rate were effective to inhibit *F. nucleatum, A. actinomycethemcomitans* and *P. gingivalis* at the first 24 h and eliminated bacterial agents from day 6 up to 18.

The study of Srithep et al. [29] also demonstrated that 6 mg fibers formed by poly(L-lactide) (PLLA)/ poly(D-lactide) (PDLA) with 10 % (w/w) MDZ presented at least 30 % (w/w) MDZ release rate at the first 12 h and the fibers had antimicrobial activity for *P. gingivalis* after 24 h, with minimal inhibitory concentration of approximately 0.5 mg/mL MDZ. In this study, 10 mg of Zein/HPMCAS fibers contain 3.46 mg of total drugs content and at least 10.53 % (w/w) drug release rate at 1 h (Table 3), which implies in a minimal drug concentration of 0.35 mg/mL considering the small amount of saliva in the pocket of the oral cavity. This drug concentration value is sufficient to inhibit bacterial growth even at the first hours of the drug release, according to the authors [25,29].

To calculate the release kinetics for BMDZ and MDZ, we considered

**Table 3**
Fitted parameters using First order, Higuchi and Korsmeyer-Peppas models to calculate the drug release kinetics. (The kinetic parameters were calculated using the entire profile, except for the Korsmeyer-Peppas model that was used up to 60 % release). The amount of the drugs in the fibers is given in % (w/w).

| Drugs release from Zein/HPMCAS fibers with and without CNF | | | | | |
|---|---|---|---|---|---|
| Model | Parameters | 40.0 % BMDZ | 40.0 % MDZ | 20.0 % BMDZ +20.0 % MDZ | 20.0 % BMDZ+ 20.0 % MDZ without CNF |
| First order | $k_1$ | $1.80 \times 10^{-4}$ | $5.00 \times 10^{-5}$ | $7.30 \times 10^{-5}$ | $3.30 \times 10^{-4}$ |
| | $R^2$ | 0.67 | 0.16 | 0.65 | 0.90 |
| Higuchi | $k_H$ | 0.95 | 0.15 | 0.40 | 0.93 |
| | $R^2$ | 0.85 | 0.20 | 0.81 | 0.87 |
| Korsmeyer-Peppas | n | 0.45 | 0.04 | 0.15 | 0.27 |
| | $k_{K\text{-}P}$ | 0.61 | 4.10 | 2.85 | 2.28 |
| | $R^2$ | **0.97** | **0.40** | **0.95** | **0.95** |
| **Individual drug release from Zein/HPMCAS fibers with 20.0 % BMDZ + 20.0 % MDZ** | | | | | |
| Model | Parameters | With CNF | | Without CNF | |
| | | 20.0 % BMDZ | 20.0 % MDZ | 20.0 % BMDZ | 20.0 % MDZ |
| First order | $k_1$ | $1.30 \times 10^{-4}$ | $2.50 \times 10^{-5}$ | $3.00 \times 10^{-4}$ | $6.40 \times 10^{-4}$ |
| | $R^2$ | 0.65 | 0.38 | 0.98 | 0.90 |
| Higuchi | $k_H$ | 0.80 | 0.13 | 1.16 | 0.73 |
| | $R^2$ | 0.83 | 0.47 | 0.98 | 0.67 |
| Korsmeyer-Peppas | n | 0.49 | 0.04 | 0.66 | **0.30** |
| | $k_{K\text{-}P}$ | 0.20 | 3.65 | 1.07 | 3.27 |
| | $R^2$ | **0.92** | **0.67** | **0.99** | **0.92** |

the four most used models, such as first order, Higuchi and Korsmeyer-Peppas, given by the equations [70–72]:

$$Q_t = 1 - e^{k_1 t} \quad (1)$$

$$Q_t = k_H \sqrt{t} \quad (2)$$

$$Q_t = k_{K-P}\, t^n \quad (3)$$

where $Q_t$ is the drug release at a given time, represented by a fractional number; $k_0$, $k_1$, $k_H$, and $k_{K\text{-}P}$ are the kinetic constants for each given model, and $n$ is the diffusion exponent. Table 3 lists the fitted parameters and regression coefficient ($R^2$) using the four models for BMDZ and MDZ release from Zein/HPMCAS electrospun fibers with and without cellulose nanofibril. The fit plots are in the Supplementary Material (Fig. SM7 and SM8).

Our findings show that the Kormeyer-Peppas model (higher $R^2$ values) was a better fit for the drug release profiles from polymeric fibers, and the release profile of mixed BMDZ and MDZ followed the same pattern as the other fibers. Moreover, the $R^2$ values for all MDZ release kinetic models of the Zein/HPMCAS/CNF fibers with 40 % MDZ were significantly low, probably due to the MDZ burst release effect.

Interestingly, for most fibers adjusted by the Korsmeyer-Peppas model, the diffusion exponent ($n$) values were <0.5, indicating that the drug release resulted from the diffusion mechanism and obeys Fick's first law, meaning that the drug molecules diffuse through Zein/HPMCAS matrix, in agreement with other studies [21,25]. Moreover, a drug diffusion coefficient of $n = 0.45$ refers to its diffusion from a cylinder, as in the BMDZ release from Zein/HPMCAS/CNF membrane with 40 % (w/w) BMDZ. Conversely, CNF-free fibers containing 20 % (w/w) BMDZ/ 20 % (w/w) MDZ presented $n > 0.5$ for individual BMDZ release, suggesting an anomalous transport mechanism (non-Fickian diffusion).

Our research reveals that Zein/HPMCAS fibers can be produced using a green, environmentally friendly solvent instead of hazardous ones [8,20,25,29,69]. Also, fibers were obtained with high amount of

BMDZ and or/ MDZ molecules, showing adequate release rate to reach the minimal inhibitory concentration of some bacterial agents. In particular, Zein/HPMCAS/PEO fibers with 20 % (w/w) BMDZ +20 % (w/w) MDZ showed the better release rate as the membranes released sufficient amount of the drugs at the first 24 h (74 % (w/w) release rate) and had a more sustained-release at long times up to 5 days (93 % (w/w)). Moreover, in thesis, the combination of BMDZ and MDZ molecules in the fibers is strategic, since a higher concentration of MDZ at the first hours maintain the concentration of the drug adequate to treat the periodontal disease, followed by an increased BMDZ release rate during 5 days, keeping the minimal concentration of the drug efficient to inhibit and or/ eliminate the pathogen agents.

Further study should be investigated aiming at obtaining fibers in the nano scale, since thinner fibers have higher surface and probably the drug release rate should be higher [29]. For this purpose, changing the ethanol/water proportions and the concentration of the polymers and the nanocellulose particles are required. Moreover, obtaining CNF-membranes with higher sustained-drug release for at least up to 21 days, with sufficient drug concentration to act as antibacterial material are desirable.

## 4. Conclusion

This study showed that electrospun fibers composed of HPMCAS-blended zein, both without and with the incorporation of cellulose nanofibrils, have the potential to effectively control the release of BMDZ and MDZ over a period of 5 days and 48 h, respectively, as confirmed by simulated release assays. Notably, the fibers formed by Zein/HPMCAS/PEO with 20 % (w/w) BMDZ and 20 % (w/w) MDZ showed an improved release profile for the intended application in periodontitis treatment. This enhancement can be attributed to the presence of nanocellulose, which contributed to a reduction in the drug release rate. Nevertheless, cellulose nanoparticles indeed played a crucial role not only in modulating drug release but also in facilitating the electrospinning process and ensuring the overall quality of the produced fibers. These platforms hold potential utility in treating periodontal pockets, where fibers with CNF can be strategically combined with those without nanoparticles to finely modulate drugs release.

## CRediT authorship contribution statement

**João O. Ferreira:** Writing – review & editing, Writing – original draft, Visualization, Validation, Methodology, Investigation, Formal analysis, Data curation. **Giovana C. Zambuzi:** Writing – review & editing, Writing – original draft, Validation, Methodology, Investigation, Formal analysis, Data curation. **Camilla H.M. Camargos:** Writing – review & editing, Writing – original draft, Visualization, Validation, Methodology, Investigation, Formal analysis, Data curation. **Ana C.W. Carvalho:** Writing – review & editing, Writing – original draft, Validation, Methodology, Investigation, Formal analysis, Data curation. **Maíra P. Ferreira:** Writing – original draft, Visualization, Validation, Methodology, Investigation, Formal analysis, Data curation. **Camila A. Rezende:** Writing – review & editing, Writing – original draft, Visualization, Formal analysis, Conceptualization. **Osvaldo de Freitas:** Writing – review & editing, Resources, Funding acquisition, Conceptualization. **Kelly R. Francisco:** Writing – review & editing, Writing – original draft, Visualization, Validation, Supervision, Resources, Project administration, Methodology, Investigation, Funding acquisition, Formal analysis, Data curation, Conceptualization.

## Declaration of competing interest

The authors declare that they have no known competing financial interests or personal relationships that could have appeared to influence the work reported in this paper.

## Data availability

Data will be made available on request.

## Acknowledgements

Research funded by FAPESP (Brazil) (2017/20006-4, 2018/23769-1, 2021/12071-6), and the National Council for Scientific and Technological Development (CNPq, grants 140558/2017-9 and 151281/2022-0). G. C. Z holds a fellowship from FAPESP (Brazil) (2018/12146-3). We thank Espaço da Escrita - Pró-Reitoria de Pesquisa - UNICAMP for the language services provided. This research used facilities of the Brazilian Biorenewables National Laboratory (LNBR), part of the Brazilian Center for Research in Energy and Materials (CNPEM), a private non-profit organization under the supervision of the Brazilian Ministry for Science, Technology, and Innovations (MCTI). The Biophysics of Macromolecules (BFM) staff is acknowledged for the assistance during the experiments (20231846).

## Appendix A. Supplementary data

Supplementary data to this article can be found online at https://doi.org/10.1016/j.ijbiomac.2024.129701.

## References

[1] G. Hajishengallis, Periodontitis: from microbial immune subversion to systemic inflammation, Nat. Rev. Immunol. 15 (2015) 30–44, https://doi.org/10.1038/nri3785.
[2] R.J. Lamont, H. Koo, G. Hajishengallis, The oral microbiota: dynamic communities and host interactions (2018), https://doi.org/10.1038/s41579-018-0089-x.
[3] A.C.S. Ré, M.P. Ferreira, O. Freitas, C.P. Aires, Antimicrobial effect of a local release system containing metronidazole against a Porphyromonas gingivalis biofilm, Pharmazie 74 (2019) 665–666, https://doi.org/10.1691/ph.2019.8241.
[4] Y. Wang, J. Deng, T. Zhang, Y. Hua, Y. Wang, Q. Zhang, T. Jiao, C. Li, X. Zhang, A study on the use of phase transition lysozyme-loaded minocycline hydrochloride in the local treatment of chronic periodontitis, ACS Appl. Bio Mater. 5 (2022) 3146–3157, https://doi.org/10.1021/acsabm.2c00079.
[5] K. Jepsen, W. Falk, F. Brune, R. Fimmers, S. Jepsen, I. Bekeredjian-Ding, Prevalence and antibiotic susceptibility trends of periodontal pathogens in the subgingival microbiota of German periodontitis patients: a retrospective surveillance study, J. Clin. Periodontol. 48 (2021) 1216–1227, https://doi.org/10.1111/jcpe.13468.
[6] A.L.R. Pavanelli, B.S. De Menezes, E.B.B. Pereira, F.A. De Souza Morais, J.A. Cirelli, R.S. De Molon, Pharmacological therapies for the management of inflammatory bone resorption in periodontal disease: a review of preclinical studies, Biomed. Res. Int. 2022 (2022), https://doi.org/10.1155/2022/5832009.
[7] N. Petrescu, B. Crisan, O. Aghiorghiesei, C. Sarosi, I.C. Mirica, O. Lucaciu, S.A.L. Iușan, N. Dirzu, D. Apostu, Gradual Drug Release Membranes and Films Used for the Treatment of Periodontal Disease, Membranes 2022, Vol. 12, Page 895. 12 (2022) 895. doi:https://doi.org/10.3390/MEMBRANES12090895.
[8] M. Budai-Szűcs, A. Léber, L. Cui, M. Józó, P. Vályi, K. Burián, B. Kirschweng, E. Csányi, B. Pukánszky, Electrospun PLA fibers containing metronidazole for periodontal disease, Drug Des. Devel. Ther. 14 (2020) 233–242, https://doi.org/10.2147/DDDT.S231748.
[9] G.R. Pitcher, H.N. Newman, J.D. Strahan, Access to subgingival plaque by disclosing agents using mouthrinsing and direct irrigation, J. Clin. Periodontol. 7 (1980) 300–308, https://doi.org/10.1111/J.1600-051X.1980.TB01972.X.
[10] J.M. Goodson, Pharmacokinetic principles controlling efficacy of oral therapy, J. Dent. Res. 68 (1989) 1625–1632.
[11] K.P. Steckiewicz, P. Cieciórski, E. Barcińska, M. Jaśkiewicz, M. Narajczyk, M. Bauer, W. Kamysz, E. Megiel, I. Inkielewicz-Stepniak, Silver nanoparticles as chlorhexidine and metronidazole drug delivery platforms: their potential use in treating periodontitis, Int. J. Nanomedicine 17 (2022) 495–517, https://doi.org/10.2147/IJN.S339046.
[12] P.C. Chang, W.C. Tai, H.T. Luo, C.H. Lai, H.H. Lin, Z.J. Lin, Y.C. Chang, B.S. Lee, Core-shell poly-(D,L-lactide-co-glycolide)-chitosan nanospheres with simvastatin-doxycycline for periodontal and osseous repair, Int. J. Biol. Macromol. 158 (2020) 627–635. doi:https://doi.org/10.1016/j.ijbiomac.2020.04.183.
[13] A.C.S. Ré, M.P. Ferreira, O. Freitas, C.P. Aires, Local antibiotic delivery in periodontitis: drug release and its effect on supragingival biofilms, Biofouling 32 (2016) 1061–1066, https://doi.org/10.1080/08927014.2016.1230735.
[14] N. Baranov, M. Popa, L.I. Atanase, D.L. Ichim, Polysaccharide-based drug delivery systems for the treatment of periodontitis, Molecules 2021, Vol. 26, Page 2735. 26 (2021) 2735. doi:https://doi.org/10.3390/MOLECULES26092735.
[15] H.N. Ho, H.H. Le, T.G. Le, T.H.A. Duong, V.Q.T. Ngo, C.T. Dang, V.M. Nguyen, T. H. Tran, C.N. Nguyen, Formulation and characterization of hydroxyethyl cellulose-based gel containing metronidazole-loaded solid lipid nanoparticles for buccal

mucosal drug delivery, Int. J. Biol. Macromol. 194 (2022) 1010–1018, https://doi.org/10.1016/j.ijbiomac.2021.11.161.
[16] L. Wang, Y. Li, M. Ren, X. Wang, L. Li, F. Liu, Y. Lan, S. Yang, J. Song, pH and lipase-responsive nanocarrier-mediated dual drug delivery system to treat periodontitis in diabetic rats, Bioact Mater. 18 (2022) 254–266, https://doi.org/10.1016/j.bioactmat.2022.02.008.
[17] M. Qi, X. Ren, W. Li, Y. Sun, X. Sun, C. Li, S. Yu, L. Xu, Y. Zhou, S. Song, B. Dong, L. Wang, NIR responsive nitric oxide nanogenerator for enhanced biofilm eradication and inflammation immunotherapy against periodontal diseases, Nano Today 43 (2022) 101447, https://doi.org/10.1016/j.nantod.2022.101447.
[18] D.M. Dos Santos, S.R. De Annunzio, J.C. Carmello, A.C. Pavarina, C.R. Fontana, D. S. Correa, Combining coaxial electrospinning and 3D printing: design of biodegradable bilayered membranes with dual drug delivery capability for periodontitis treatment, ACS Appl Bio Mater. 5 (2022) 146–159, https://doi.org/10.1021/acsabm.1c01019.
[19] Y. Ma, J. Song, H.N.S. Almassri, D. Zhang, T. Zhang, Y. Cheng, X. Wu, Minocycline-loaded PLGA electrospun membrane prevents alveolar bone loss in experimental peridontitis, Drug Deliv. 27 (2020) 151–160, https://doi.org/10.1080/10717544.2019.1709921.
[20] M. Zamani, M. Morshed, J. Varshosaz, M. Jannesari, Controlled release of metronidazole benzoate from poly ε-caprolactone electrospun nanofibers for periodontal diseases, Eur. J. Pharm. Biopharm. 75 (2010) 179–185, https://doi.org/10.1016/j.ejpb.2010.02.002.
[21] J.A. Ferreira, K.Z. Kantorski, N. Dubey, A. Daghrery, J.C. Fenno, Y. Mishina, H. L. Chan, G. Mendonça, M.C. Bottino, Personalized and defect-specific antibiotic-laden scaffolds for periodontal infection ablation, ACS Appl. Mater. Interfaces 13 (2021) 49642–49657, https://doi.org/10.1021/acsami.1c11787.
[22] I.C. Mirică, G. Furtos, O. Lucaciu, P. Pascuta, M. Vlassa, M. Moldovan, R. S. Campian, Electrospun membranes based on polycaprolactone, nano-hydroxyapatite and metronidazole, Materials 14 (2021) 1–13, https://doi.org/10.3390/ma14040931.
[23] J. Xue, M. He, Y. Niu, H. Liu, A. Crawford, P. Coates, D. Chen, R. Shi, L. Zhang, Preparation and in vivo efficient anti-infection property of GTR/GBR implant made by metronidazole loaded electrospun polycaprolactone nanofiber membrane, Int. J. Pharm. 475 (2014) 566–577, https://doi.org/10.1016/j.ijpharm.2014.09.026.
[24] M. He, H. Jiang, R. Wang, Y. Xie, C. Zhao, Fabrication of metronidazole loaded poly (ε-caprolactone)/zein core/shell nanofiber membranes via coaxial electrospinning for guided tissue regeneration, J. Colloid Interface Sci. 490 (2017) 270–278, https://doi.org/10.1016/j.jcis.2016.11.062.
[25] M. Reise, R. Wyrwa, U. Müller, M. Zylinski, A. Völpel, M. Schnabelrauch, A. Berg, K.D. Jandt, D.C. Watts, B.W. Sigusch, Release of metronidazole from electrospun poly(l-lactide-co-d/l-lactide) fibers for local periodontitis treatment, Dent. Mater. 28 (2012) 179–188, https://doi.org/10.1016/j.dental.2011.12.006.
[26] F. Notario-Pérez, A. Martín-Illana, R. Cazorla-Luna, R. Ruiz-Caro, L.M. Bedoya, J. Peña, M.D. Veiga, Development of mucoadhesive vaginal films based on HPMC and zein as novel formulations to prevent sexual transmission of HIV, Int. J. Pharm. 570 (2019) 118643, https://doi.org/10.1016/j.ijpharm.2019.118643.
[27] H. Van Ngo, P.K. Nguyen, T. Van Vo, W. Duan, V.T. Tran, P.H.L. Tran, T.T.D. Tran, Hydrophilic-hydrophobic polymer blend for modulation of crystalline changes and molecular interactions in solid dispersion, Int. J. Pharm. 513 (2016) 148–152, https://doi.org/10.1016/j.ijpharm.2016.09.017.
[28] T. Lin, C. Lu, L. Zhu, T. Lu, The biodegradation of zein in vitro and in vivo and its application in implants, AAPS PharmSciTech 12 (2011) 172, https://doi.org/10.1208/S12249-010-9565-Y.
[29] Y. Srithep, T. Akkaprasa, D. Pholharn, J. Morris, S.J. Liu, P. Patrojanasophon, T. Ngawhirunpat, Metronidazole-loaded polylactide stereocomplex electrospun nanofiber mats for treatment of periodontal disease, J Drug Deliv Sci Technol. 64 (2021) 102582, https://doi.org/10.1016/j.jddst.2021.102582.
[30] K. Nazari, E. Kontogiannidou, R.H. Ahmad, A. Gratsani, M. Rasekh, M.S. Arshad, B. S. Sunar, D. Armitage, N. Bouropoulos, M.W. Chang, X. Li, D.G. Fatouros, Z. Ahmad, Development and characterisation of cellulose based electrospun mats for buccal delivery of non-steroidal anti-inflammatory drug (NSAID), Eur. J. Pharm. Sci. 102 (2017) 147–155, https://doi.org/10.1016/j.ejps.2017.02.033.
[31] Q. Wang, D.G. Yu, L.L. Zhang, X.K. Liu, Y.C. Deng, M. Zhao, Electrospun hypromellose-based hydrophilic composites for rapid dissolution of poorly water-soluble drug, Carbohydr. Polym. 174 (2017) 617–625, https://doi.org/10.1016/j.carbpol.2017.06.075.
[32] A. Balogh, B. Farkas, Á. Pálvölgyi, A. Domokos, B. Démuth, G. Marosi, Z.K. Nagy, Novel alternating current electrospinning of hydroxypropylmethylcellulose acetate succinate (HPMCAS) nanofibers for dissolution enhancement: the importance of solution conductivity, J. Pharm. Sci. 106 (2017) 1634–1643, https://doi.org/10.1016/j.xphs.2017.02.021.
[33] H. Li, B. Sanchez-Vazquez, R.P. Trindade, Q. Zou, Y. Mai, L. Dou, L.M. Zhu, G. R. Williams, Electrospun oral formulations for combined photo-chemotherapy of colon cancer, Colloids Surf. B: Biointerfaces 183 (2019) 110411, https://doi.org/10.1016/j.colsurfb.2019.110411.
[34] A. Kazsoki, B. Palcsó, A. Alpár, R. Snoeck, G. Andrei, R. Zelkó, Formulation of acyclovir (core)-dexpanthenol (sheath) nanofibrous patches for the treatment of herpes labialis, Int. J. Pharm. 611 (2022), https://doi.org/10.1016/j.ijpharm.2021.121354.
[35] N. Hasan, L. Rahman, S.H. Kim, J. Cao, A. Arjuna, S. Lallo, B.H. Jhun, J.W. Yoo, Recent advances of nanocellulose in drug delivery systems, J. Pharm. Investig. 50 (2020) 553–572, https://doi.org/10.1007/s40005-020-00499-4.
[36] A.B. Meneguin, B. Stringhetti, F. Cury, A.M. Dos Santos, D. Faza Franco, H. S. Barud, E.C. Da, S. Filho, Resistant starch/pectin free-standing films reinforced with nanocellulose intended for colonic methotrexate release, Carbohydr. Polym. 157 (2017) 1013–1023, https://doi.org/10.1016/j.carbpol.2016.10.062.
[37] A. Sheikhi, J. Hayashi, J. Eichenbaum, M. Gutin, N. Kuntjoro, D. Khorsandi, A. Khademhosseini, Recent advances in nanoengineering cellulose for cargo delivery, J. Control. Release 294 (2019) 53, https://doi.org/10.1016/J.JCONREL.2018.11.024.
[38] G.C. Zambuzi, C.H.M. Camargos, M.P. Ferreira, C.A. Rezende, O. de Freitas, K. R. Francisco, Modulating the controlled release of hydroxychloroquine mobilized on pectin films through film-forming pH and incorporation of nanocellulose, Carbohydrate Polymer Technologies and Applications 2 (2021) 100140, https://doi.org/10.1016/j.carpta.2021.100140.
[39] C.H.M. Camargos, C.A. Rezende, Structure-property relationships of cellulose nanocrystals and nanofibrils: implications for the design and performance of nanocomposites and all-nanocellulose systems, ACS Appl Nano Mater. 4 (2021) 10505–10518, https://doi.org/10.1021/acsanm.1c02008.
[40] Z. Pedram Rad, J. Mokhtari, M. Abbasi, Biopolymer based three-dimensional biomimetic micro/nanofibers scaffolds with porous structures via tailored charge repulsions for skin tissue regeneration, Polym. Adv. Technol. 32 (2021) 3535–3548, https://doi.org/10.1002/pat.5364.
[41] Y.H. Wang, M. Zhao, S.A. Barker, P.S. Belton, D.Q.M. Craig, A spectroscopic and thermal investigation into the relationship between composition, secondary structure and physical characteristics of electrospun zein nanofibers, Mater. Sci. Eng. C 98 (2019) 409–418, https://doi.org/10.1016/j.msec.2018.12.134.
[42] P.M. Silva, C. Prieto, J.M. Lagarón, L.M. Pastrana, M.A. Coimbra, A.A. Vicente, M. A. Cerqueira, Food-grade hydroxypropyl methylcellulose-based formulations for electrohydrodynamic processing: part I – role of solution parameters on fibre and particle production, Food Hydrocoll. 118 (2021). doi:https://doi.org/10.1016/j.foodhyd.2021.106761.
[43] A. Balogh, B. Farkas, G. Verreck, J. Mensch, E. Borbás, B. Nagy, G. Marosi, Z. K. Nagy, AC and DC electrospinning of hydroxypropylmethylcellulose with polyethylene oxides as secondary polymer for improved drug dissolution, Int. J. Pharm. 505 (2016) 159–166, https://doi.org/10.1016/j.ijpharm.2016.03.024.
[44] A. Aydogdu, G. Sumnu, S. Sahin, A novel electrospun hydroxypropyl methylcellulose/polyethylene oxide blend nanofibers: morphology and physicochemical properties, Carbohydr. Polym. 181 (2018) 234–246, https://doi.org/10.1016/j.carbpol.2017.10.071.
[45] S. Torres-Giner, E. Gimenez, J.M. Lagaron, Characterization of the morphology and thermal properties of Zein Prolamine nanostructures obtained by electrospinning, Food Hydrocoll. 22 (2008) 601–614, https://doi.org/10.1016/j.foodhyd.2007.02.005.
[46] A. Altan, Ö. Çayır, Encapsulation of carvacrol into ultrafine fibrous zein films via electrospinning for active packaging, Food Packag. Shelf Life 26 (2020), https://doi.org/10.1016/j.fpsl.2020.100581.
[47] M.A. Miri, M.B. Habibi Najafi, J. Movaffagh, B. Ghorani, Encapsulation of ascorbyl palmitate in zein by electrospinning technique, J. Polym. Environ. 29 (2021) 1089–1098, https://doi.org/10.1007/s10924-020-01954-x.
[48] K. Kanjanapongkul, S. Wongsasulak, T. Yoovidhya, Investigation and prevention of clogging during electrospinning of zein solution, J. Appl. Polym. Sci. 118 (2010) 1821–1829, https://doi.org/10.1002/app.32499.
[49] Y. Wu, J. Du, J. Zhang, Y. Li, Z. Gao, pH effect on the structure, rheology, and electrospinning of maize Zein, Foods 12 (2023), https://doi.org/10.3390/foods12071395.
[50] M. Wang, D. Li, J. Li, S. Li, Z. Chen, D.G. Yu, Z. Liu, J.Z. Guo, Electrospun Janus zein–PVP nanofibers provide a two-stage controlled release of poorly water-soluble drugs, Mater. Des. 196 (2020) 109075, https://doi.org/10.1016/j.matdes.2020.109075.
[51] M. Aratono, T. Toyomasu, M. Villeneuve, Y. Uchizono, T. Takiue, K. Motomura, N. Ikeda, Thermodynamic Study on the Surface Formation of the Mixture of Water and Ethanol, 1997.
[52] S. Shukla, E. Brinley, H.J. Cho, S. Seal, Electrospinning of hydroxypropyl cellulose fibers and their application in synthesis of nano and submicron tin oxide fibers, Polymer (Guildf). 46 (2005) 12130–12145, https://doi.org/10.1016/j.polymer.2005.10.070.
[53] H. Chen, J. Chen, N. Teng, H. Na, J. Zhu, Controlling the status of corn cellulose solutions by ethanol to define fiber morphology during electrospinning, Cellulose 24 (2017) 863–870, https://doi.org/10.1007/s10570-016-1127-3.
[54] S. Tungprapa, T. Puangparn, M. Weerasombut, I. Jangchud, P. Fakum, S. Semongkhol, C. Meechaisue, P. Supaphol, Electrospun cellulose acetate fibers: effect of solvent system on morphology and fiber diameter, Cellulose 14 (2007) 563–575, https://doi.org/10.1007/s10570-007-9113-4.
[55] C.M. Phan, The surface tension and interfacial composition of water/ethanol mixture, J. Mol. Liq. 342 (2021), https://doi.org/10.1016/j.molliq.2021.117505.
[56] B. Niu, L. Zhan, P. Shao, N. Xiang, P. Sun, H. Chen, H. Gao, Electrospinning of zein-ethyl cellulose hybrid nanofibers with improved water resistance for food preservation, Int. J. Biol. Macromol. 142 (2020) 592–599, https://doi.org/10.1016/j.ijbiomac.2019.09.134.
[57] D.C. Morse, Viscoelasticity of Tightly Entangled Solutions of Semiflexible Polymers, 1998.
[58] K.R. Francisco, M.A. da Silva, E. Sabadini, G. Karlsson, C.A. Dreiss, Effect of monomeric and polymeric co-solutes on cetyltrimethylammonium bromide wormlike micelles: rheology, Cryo-TEM and small-angle neutron scattering, J. Colloid Interface Sci. 345 (2010) 351–359, https://doi.org/10.1016/j.jcis.2010.01.086.
[59] O.A. Hisseine, N. Basic, A.F. Omran, A. Tagnit-Hamou, Feasibility of using cellulose filaments as a viscosity modifying agent in self-consolidating concrete, Cem. Concr.

Compos. 94 (2018) 327–340, https://doi.org/10.1016/j.cemconcomp.2018.09.009.
[60] A.B. Perumal, R.B. Nambiar, J.A. Moses, C. Anandharamakrishnan, Nanocellulose: recent trends and applications in the food industry, Food Hydrocoll. 127 (2022), https://doi.org/10.1016/j.foodhyd.2022.107484.
[61] D.J. Mendoza, L. Hossain, C. Browne, V.S. Raghuwanshi, G.P. Simon, G. Garnier, Controlling the transparency and rheology of nanocellulose gels with the extent of carboxylation, Carbohydr. Polym. 245 (2020), https://doi.org/10.1016/j.carbpol.2020.116566.
[62] K. Heise, E. Kontturi, Y. Allahverdiyeva, T. Tammelin, M.B. Linder, O. Ikkala Nonappa, Nanocellulose: recent fundamental advances and emerging biological and biomimicking applications, Adv. Mater. 33 (2021) 2004349, https://doi.org/10.1002/adma.202004349.
[63] T. Moberg, K. Sahlin, K. Yao, S. Geng, G. Westman, Q. Zhou, K. Oksman, M. Rigdahl, Rheological properties of nanocellulose suspensions: effects of fibril/particle dimensions and surface characteristics, Cellulose 24 (2017) 2499–2510, https://doi.org/10.1007/s10570-017-1283-0.
[64] L.C. Malucelli, M. Matos, C. Jordão, L.G. Lacerda, M.A.S. Carvalho Filho, W.L. E. Magalhães, Grinding severity influences the viscosity of cellulose nanofiber (CNF) suspensions and mechanical properties of nanopaper, Cellulose 25 (2018) 6581–6589, https://doi.org/10.1007/s10570-018-2031-9.
[65] B. Li, L.A. Wegiel, L.S. Taylor, K.J. Edgar, Stability and solution concentration enhancement of resveratrol by solid dispersion in cellulose derivative matrices, Cellulose 20 (2013) 1249–1260, https://doi.org/10.1007/s10570-013-9889-3.
[66] M.R. Caira, L.R. Nassimbeni, B. van Oudtshoorn, X-ray structural characterization of anhydrous metronidazole benzoate and metronidazole benzoate monohydrate, J. Pharm. Sci. 82 (1993) 1006–1009, https://doi.org/10.1002/jps.2600821003.
[67] H.T.T. Dinh, P.H.L. Tran, W. Duan, B.J. Lee, T.T.D. Tran, Nano-sized solid dispersions based on hydrophobic-hydrophilic conjugates for dissolution enhancement of poorly water-soluble drugs, Int. J. Pharm. 533 (2017) 93–98, https://doi.org/10.1016/j.ijpharm.2017.09.065.
[68] E. Corradini, P.S. Curti, A.B. Meniqueti, A.F. Martins, A.F. Rubira, E.C. Muniz, Recent advances in food-packing, pharmaceutical and biomedical applications of zein and zein-based materials, Int. J. Mol. Sci. 15 (2014) 22438–22470, https://doi.org/10.3390/ijms151222438.
[69] D. Schkarpetkin, M. Reise, R. Wyrwa, A. Völpel, A. Berg, M. Schweder, M. Schnabelrauch, D.C. Watts, B.W. Sigusch, Development of novel electrospun dual-drug fiber mats loaded with a combination of ampicillin and metronidazole, Dent. Mater. 32 (2016) 951–960, https://doi.org/10.1016/j.dental.2016.05.002.
[70] R.W. Korsmeyer, R. Gurny, E. Doelker, P. Buri, N.A. Peppas, Mechanisms of solute release from porous hydrophilic polymers, Int. J. Pharm. 15 (1983) 25–35, https://doi.org/10.1016/0378-5173(83)90064-9.
[71] N.A. Peppas, A.R. Khare, Preparation, structure and diffusional behavior of hydrogels in controlled release, Adv. Drug Deliv. Rev. 11 (1993) 1–35, https://doi.org/10.1016/0169-409X(93)90025-Y.
[72] P. Costa, J.M. Sousa Lobo, Modeling and comparison of dissolution profiles, Eur. J. Pharm. Sci. 13 (2001) 123–133, https://doi.org/10.1016/S0928-0987(01)00095-1.